ACS Macro Letters

Letter

pubs.acs.org/macroletters

Investigation of the Local Environment of Hydrophobic End Groups on Polyethylene Glycol (PEG) Brushes Using Fluorometry: Relationship to Click Chemistry Conjugation Reactions on PEG-Protected Nanoparticles

Christopher V. H.-H. Chen, Brian P. Triana, and Robert K. Prud'homme*

Department of Chemical and Biological Engineering, Princeton University, Princeton, New Jersey 08540, United States

Supporting Information

ABSTRACT: Targeted nanoparticles often require conjugating targeting ligands to polyethylene glycol (PEG) chains of a nanoparticle's dense protecting corona. "Click" chemistries are commonly employed for their bioorthogonality, with strain-promoted azide−alkyne cycloadditions (SPAAC) increasingly chosen to avoid cytotoxic copper catalysts. However, conjugation becomes compromised if reactive PEG chain ends cannot encounter their reaction counterparts. We use fluorescence to probe the location of Nile Red, methylpyrene, and butylpyrene, dyes with comparable hydrophobicities to SPAAC alkynes (logP = 3.2−5.7), tethered to PEG chains on 100 nm NPs. Using fluorescence peak shifts, we find that Nile Red resides 43% of the time in the 5k PEG corona and 57% at the more hydrophobic nanoparticle core. Increasing the PEG MW to 67k doubles the corona dye fraction to 86% (14% core). More hydrophobic methylpyrene and butylpyrene, monitored with I1/I3 ratios, reside 1% in the corona (99% core). These results explain difficulties with using SPAAC reactions for conjugating large ligands to nanoparticles with PEG coronae.

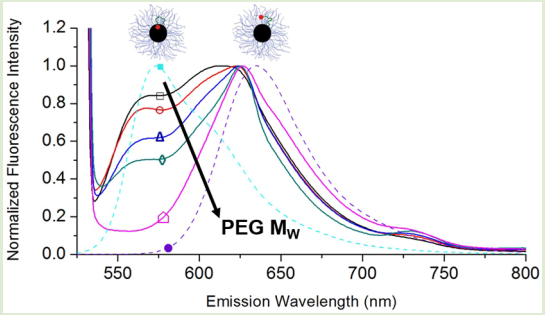

Most nanoparticle (NP) constructs for biomedical applications have polyethylene glycol (PEG) coatings due to the coating's ability to decrease nonspecific protein adsorption to the NP, increase circulation time, and prevent opsonization by the reticuloendothelial system (RES).[1] These NPs may be modified, or "targeted," to interact with receptors on cells, tissues, or organs. Optimally, targeted NPs have dense surface PEG layers to prevent RES clearance, with specific targeting ligands presented on their surfaces to bind to receptors. Often, the targeting ligands are reacted onto the ends of PEG chains after NP synthesis. If the targeting ligand is large, antibodies (MW ∼ 150k), single chain antibody fragments (MW ∼ 10−15k), or proteins, the steric interactions between the ligand and the PEG brush layer may significantly decrease the conjugation reaction kinetics relative to small molecule ligands. This arises from the inability of larger ligands to interact with the PEG chain ends, which are distributed throughout the PEG brush layer.[2]

A variety of conjugation reactions have been used to connect PEG chains to ligands. Of particular interest are "click" (azide−alkyne Huisgen cycloaddition) reactions, most commonly copper(I)-catalyzed azide−alkyne cycloaddition (CuAAC), that has grown in use dramatically due to the reaction's bioorthogonality and high regioselectivity in aqueous media.[3] Some concern over the cytotoxicity of the copper(I) catalyst has led to the development of copper-free "click" chemistries for in vivo applications.[4] Strain-promoted azide−alkyne cycloaddition (SPAAC) is a common example of copper-free "click", which uses ring-strain to activate the alkyne. SPAAC alkynes include dibenzocyclooctynes (DBCO), bicyclo-[6.1.0]-nonyne (BCN), and difluorinated cyclooctyne 2 (DIFO2),[5] which are commercially available. These are relatively hydrophobic with octanol−water partition coefficients (logPs) as shown in Table 1 (molecular structures in the Supporting Information).

In our experience, using SPAAC alkynes on 5k PEG chains in dense brush layers to couple 14k antibody fragments onto our polymeric NPs for targeting has been problematic. To the authors' knowledge there are no examples of successful protein conjugation using SPAAC alkynes to the surface of PEG-protected polymer nanoparticles. Since the mechanism for SPAAC requires the interaction between cycloalkyne and azide,[6] we hypothesize that a bias in the distribution of these hydrophobic functional end groups toward the hydrophobic core, and away from the NP corona−water interface, causes a drop in the reaction efficiency relative to the reaction in free solution. The problem is demonstrated graphically in Figure 1, for the three cases of ligand conjugation: neutral PEG end-small ligand, neutral PEG end-large ligand, and hydrophobic PEG end-large ligand. For the first two cases (Figure 1A,B), we plot the distributions of chain ends, as presented by Milner et al.,[7]

Received: February 13, 2015
Accepted: April 14, 2015
Published: April 20, 2015

DOI: 10.1021/acsmacrolett.5b00119
ACS Macro Lett. 2015, 4, 521−525

Table 1. Comparison of Octanol–Water Partition Coefficients (logPs)[a] of Functional End Groups[b]

end group	log *P*
alkyne	0.3
azide	0.9
DBCO[c]	2.9
BCN[d]	3.0
Nile Red (NR)	3.2
DIFO2[e]	4.3
methylpyrene (PyM)	4.4
butylpyrene (PyB)	5.7

[a]Calculated via Molinspiration software by Cheminformatics. Available from http://molinspiration.com. [b]Structures in the Supporting Information. [c]Dibenzocyclooctyne. [d]Bicyclo-[6.1.0]-nonyne. [e]Difluorinated cyclooctyne.

from simulations of self-avoiding walks of chains in a brush layer. Since our NPs are around 100 nm in diameter and our PEG brush layers have thicknesses around 10–20 nm,[8] we represent these PEG brushes on flat plates since particle sizes are much larger than brush thickness. For smaller polymeric micelles, curvature might make a quantitative, but not qualitative, difference to this picture. These end groups have no specific interaction with the surface, and we denote these as "neutral ends." Small ligands, such as small molecule dyes, can permeate the PEG layer, attain a constant concentration throughout the layer, and allow the conjugation to proceed without any additional resistance. Large ligands, such as proteins, have to push into the PEG layer to react with the functional chain end. Additional work (osmotic pressure multiplied by the displaced volume of the PEG layer) needed to displace the PEG corona decreases the protein concentration in the brush and decreases the probability of the reaction between the chain end and the reactive moiety on the ligand (Figure 1B).

Figure 1C shows the third case, where a large ligand is to be conjugated with a hydrophobic PEG end, such as in protein conjugation to NPs with SPAAC cycloalkynes. Since the hydrophobic end group biases the chain end toward the NP core, the probability of the chain end and the ligand interacting is decreased greatly. Consequently, the reaction efficiency would be dramatically reduced. This is consistent with our observations.

To test this hypothesis, we designed experiments to probe the microenvironment of the PEG chain ends corresponding to chains with SPAAC reactants with varying degrees of

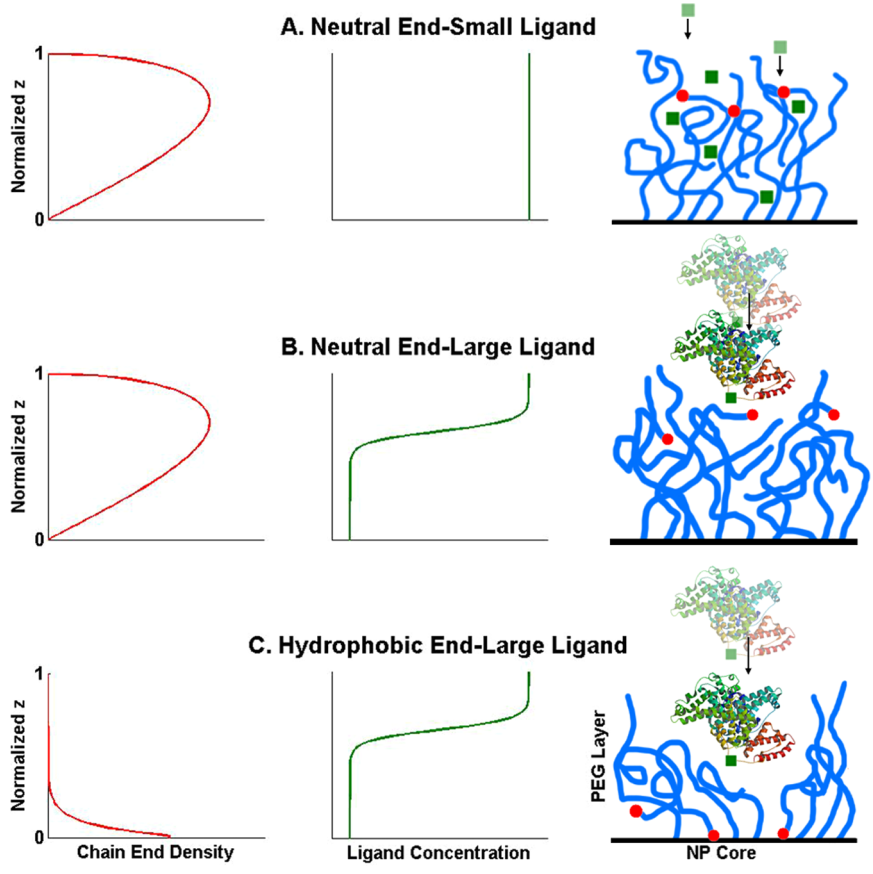

Figure 1. Graphical representation of ligands reacting with functional chain ends in a PEG layer. (A) Conjugation of a neutral chain end (that does not bias the chain end toward the NP core or surface, as described by Milner et al.[7]) with a small ligand that can permeate the PEG layer. The concentration of small ligands (green squares) is uniform, leading to reaction independent of the functional chain end's location (red circles) within the PEG layer. (B) Conjugation of a neutral chain end with a large ligand (i.e., protein). Steric repulsion diminishes the concentration of the ligand in the brush layer resulting in a decreased conjugation efficiency (green squares, represent the click group on the targeting protein) and the functional chain end, resulting in a small decrease in conjugation efficiency. (C) Conjugation of a hydrophobic chain end with a large ligand. The chain end distribution is biased toward the NP core. Hence, the joint probability of the reactive chain end and the large ligand interacting is significantly diminished, compromising the conjugation efficiency.

DOI: 10.1021/acsmacrolett.5b00119
ACS Macro Lett. 2015, 4, 521–525

hydrophobicity. Two hydrophobic fluorescent dyes were conjugated to the PEG ends on 100 nm NPs: Nile Red (NR) and pyrene (Py). Both of these dyes have environmentally sensitive fluorescent emission spectra that allow for their use as environmental indicators.[9] NPs were assembled via Flash NanoPrecipitation (FNP) using a two-inlet confined impinging jet (CIJ) mixer, as described by Han et al.[10] (Full details of dye conjugation and NP synthesis are in the Supporting Information.) The ratio of the fluorescent PEG to hydroxy-terminated PEG was chosen to be dilute enough to avoid self-quenching the dyes. Differences in fluorescence allow for the discrimination of dye location between three potential environments in/on polymeric nanoparticles, as depicted in Figure 2: at the PS core (A), in the PEG corona (B), or at the aqueous interface outside the corona (C). We determined the effect of PEG MW on the surface presentation of dye in PS–PEG NPs by conducting experiments with PS–PEG PEG blocks of 5.5k, 16.6k, 25k, 36k, and 67k with a constant 3.6k PS block.

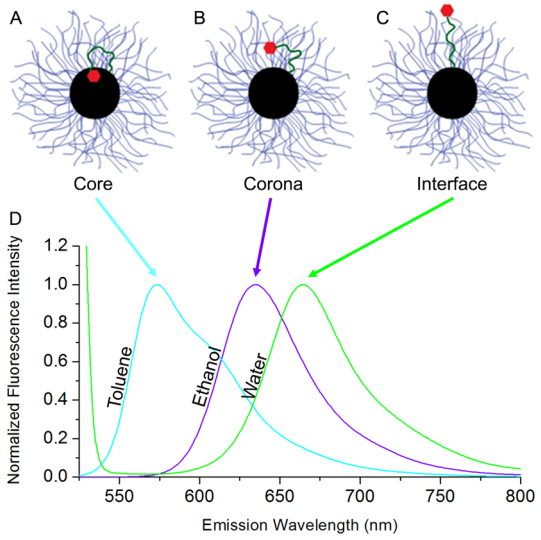

Figure 2. Three potential dye environments: (A) polystyrene NP core (black circle), (B) PEG corona (blue lines), and (C) corona–aqueous interface. The red hexagon represents the end-group modification on PS–PEG (green line) whose local environment is to be probed. (D) Normalized Nile Red emission spectra of 1 μg/mL dye in toluene (PS core-like, light blue line), ethanol (PEG corona-like, purple line) and 1 mg/mL 5k Nile Red-functionalized poly(ethylene glycol) in water (green line).

ANALYSIS OF SPECTRAL SHIFTS WITH NILE RED

Emission spectra of NR was measured in toluene, ethanol, and water to represent the PS core (Figure 2A), PEG corona (Figure 2B), and the aqueous environment at the outer boundary of the PEG corona (Figure 2C), respectively. Figure 2D shows the normalized emission spectra of NR in these solvents excited at 514 nm. Toluene and ethanol are chosen as approximations of the core and corona, respectively, due to their similarity to styrene and ethylene glycol, and are expected to yield similar NR fluorescence to their NP analogues (as demonstrated in Figure 3). The appropriateness of these approximations are discussed in the Supporting Information (SI–VII). Nile Red-functionalized (5k) PEG (PEG-NR) is used instead of pure NR in water due to the dye's low aqueous solubility. The large differences between the maximum emission wavelengths of NR in these environments, 95 nm between toluene and water and 64 nm between toluene and ethanol, allow for the discrimination of dye environment by emission spectra deconvolution. Solvation also affects NR's fluorescence intensity; the intensity is 10% lower in ethanol relative to toluene (Figure S5). Normalized fluorescence data are presented to facilitate the determination of NR environment. Non-normalized data are in the Supporting Information (Figure S6).

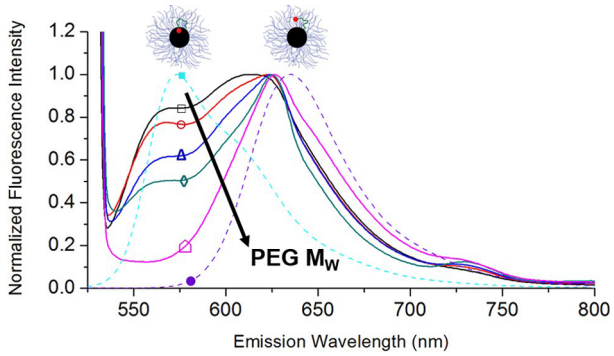

Figure 3. Normalized emission spectra of 0.1 wt % NR-tethered NPs synthesized with 1.8k PS and PS–PEG copolymer stabilizer of 3.6k PS MW and PEG MWs of 5.5k (black open square), 16.6k (red open circle), 25k (blue open triangle), 36k (green open diamond), and 67k (pink open pentagon). The dotted lines show comparison normalized spectra for NR in toluene (light blue closed square) and ethanol (purple closed circle), representing the core and corona NP environments. Increasing the PS–PEG PEG MW increases the ratio of dye in the corona vs the core.

Increasing the molecular weight of the PEG block of the PS–PEG copolymer decreases the NR concentration in the "core-like" environment, while the corona-like population increases, as shown in Figure 3. NR-tethered PEG does not emit a noticeable peak at 664 nm, indicating only a negligible amount of dye in the aqueous phase. Instead, most of the dye resides in the PEG corona and the PS core. At greater PEG block molecular weights, the corona volume increases; hence, if the NR is partitioning between the core and corona, more NR is solubilized in the corona. Fluorescence shows that a greater fraction of NR resides in the corona with increased the PEG block MW.

We can quantitatively analyze the probability of finding the functionalized chain end by deconvoluting the emission spectra using the peaks from each of the NP environments, core, corona, and corona–aqueous interface. We approximate the response as a linear superposition:

$$I_{conv} = a_{core} I_{tol} + a_{corona} I_{EtOH} + a_{aqueous} I_{water}$$

where I_{conv} is the convolved fluorescence spectra, I_{tol}, I_{EtOH}, I_{water}, are spectra representing the NP core, corona, and corona–aqueous interface, as in Figure 3, and a_{core}, a_{corona}, and $a_{aqueous}$ are constants that we use to weight the relative contributions of the core, corona, and corona–aqueous interface spectra. Optimal fitting parameters for maximizing R^2 between the normalized model and experimental spectra were determined. The relative amount of NR in each environment is obtained from the weighting coefficients (detailed in the Supporting Information).

Figure 4 shows the relative concentration of NR in each environment as the PEG block Mw increases. For all NPs,

DOI: 10.1021/acsmacrolett.5b00119
ACS Macro Lett. 2015, 4, 521–525

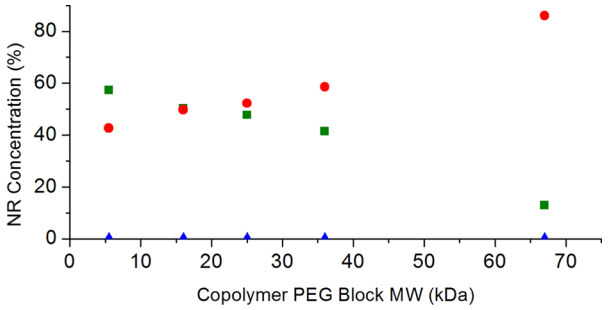

Figure 4. Percentage of NR fluorescing in the PS core (green square), PEG corona (red circle), and corona-aqueous interface (blue triangle) vs the PEG block MW. As the PEG block MW increases, a greater proportion of NR is found in the corona. The fluorescence corresponding to dye in the aqueous environment is insignificant.

$a_{aqueous}$ is approximately zero for all PEG MWs, suggesting that the tethered NR infrequently samples the corona−aqueous interface relative to the core and corona. As the PEG block MW increases from 5.5k to 67k, the percent of NR in the corona doubles from 43% to 86%.

ANALYSIS OF POLARITY PARAMETER WITH PYRENE

A second fluorescence technique to assess the location of the functionalized PEG chain end is based on the ratio of Py's primary and tertiary fluorescence peaks (I_1/I_3, the polarity parameter), which decreases as the hydrophobicity of the dye's local environment increases.[9b,11] For this, 1-pyrenemethanol and 1-pyrenebutanol were conjugated to PS−PEG to create functional chain ends with logPs of 4.4 and 5.7, respectively (details of synthesis in the Supporting Information). These two end groups, with NR, span the hydrophobicities covered by the strained alkynes used for SPAAC in Table 1.

Figure 5 shows the polarity parameter for 0.01 mg/mL solutions of the Py derivatives in binary mixtures of ethanol and toluene. The polarity parameters of the Py derivatives tethered on PEG chains on the NP surfaces are also shown on the figure. With 100% toluene representing the polarity of the core and 100% ethanol representing the polarity of the corona, we find that the pyrene end groups are predominantly in the core. Methylpyrene (PyM) is found only 0.83% in the corona, found by interpolating between 0 and 5% ethanol in toluene. The more hydrophobic butylpyrene (PyB) is found essentially completely in the core. The lower polarity parameter of PyB-tethered NPs stems from specific interactions between polystyrene in the core and the dye generates a more hydrophobic environment than toluene (discussed further in the Supporting Information). When compared to the NR-tethered NP, for which 50% of the end groups are in the corona, we observe that increasing the hydrophobicity of the end group, such as the Py derivatives, decreases the proportion of the end group in the corona and increases the end group's population in the core.

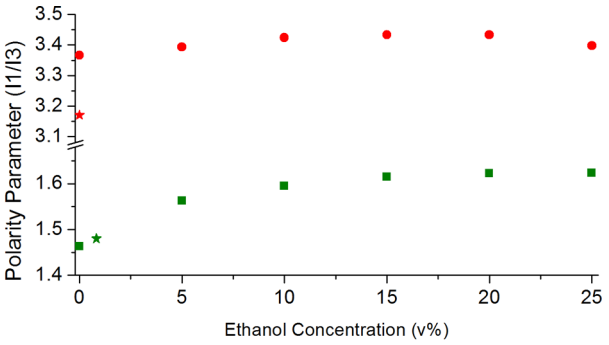

Figure 5. Polarity parameters (I_1/I_3) of 0.01 mg/mL 1-pyrenemethanol (green square) and 1-pyrenebutanol (red circle) in solutions of ethanol in toluene, compared to the polarity parameters of 0.1 wt % methylpyrene-tethered NPs (green star, polarity parameter of 1.48) and butylpyrene-tethered NPs (red star, polarity parameter of 3.17) in water. NPs were composed of 1.8k PS core and 3.6k-*b*-16.6k PS−PEG as the stabilizing block copolymer. The NP measurements indicate the more hydrophobic butylpyrene terminal group (logP = 5.7) only samples the core, and the less hydrophobic methylpyrene (logP = 4.4) samples the corona only 0.83% of the time.

By using NR and Py derivatives as fluorescent probes to determine local environments, we were able to determine that hydrophobic end groups on PEG chains sample the hydrophobic core of the nanoparticles. The fraction of the groups in the corona depends on the hydrophobicity of the terminal group and the molecular weight of the PEG chains comprising the brush. For groups with the hydrophobicity of the strained alkynes currently used in copper-free click reactions (such as for SPAAC), the fraction of chain ends in the corona would be predicted to vary from 50% for NR with the hydrophobicity of DBCO, to 0.83% for PyM with the hydrophobicity of DIFO2. The fraction of chain ends in the corona also increases with the PEG block MW from 43%, for a 5.5k PEG block, to 86%, for a 67k PEG block.

These results help to explain the difficulties encountered when using SPAAC to conjugate proteins and antibodies with ring-strained alkyne-functionalized PS−PEG NPs. This would also explain why the reactivity toward small molecule fluorophores is less sensitive to the polarity of the terminal PEG group because these small molecules can permeate the PEG corona. These results might also indicate that placing SPAAC alkynes on the ligand and the azide on the PEG chains may be a better strategy to conjugate proteins and antibodies onto NPs than the reverse. Currently we are conducting those experiments to quantify the effects of alkyne and azide "polarity" on conjugation efficiency.

ASSOCIATED CONTENT

Supporting Information

Additional information regarding the calculation of log *Ps*; synthesis of the dye-tethered copolymers; NP synthesis and formulation; material characterization; deconvolution methods; and details and further comments on fluorescence data. This material is available free of charge via the Internet at http://pubs.acs.org.

AUTHOR INFORMATION

Corresponding Author

*E-mail: prudhomm@princeton.edu. Tel.: 609-258-0211. Fax: 609-258-0211.

Notes

The authors declare no competing financial interest.

ACKNOWLEDGMENTS

This research was made possible by funding through BP/The Gulf of Mexico Research Initiative and NIH 1R01AI117776-01. We acknowledge Dr. Nathalie M. Pinkerton, Vikram J. Pansare,

DOI: 10.1021/acsmacrolett.5b00119
ACS Macro Lett. 2015, 4, 521−525

Robert F. Pagels, and Brian K. Wilson for valuable discussions. We would also like to thank Dr. Rodney D. Priestley for TGA access.

REFERENCES

(1) Davis, M. E.; Chen, Z.; Shin, D. M. *Nat. Rev.* **2008**, *7*, 771−782.
(2) Grest, G. S.; Murat, M. *Macromolecules* **1993**, *26*, 3108−3117.
(3) (a) Lutz, J.-F.; Zarafshani, Z. *Adv. Drug Delivery Rev.* **2008**, *60* (9), 958−970. (b) He, H.; Gao, C. *Curr. Org. Chem.* **2011**, *15*, 3667−3691.
(4) Baskin, J. M.; Prescher, J. A.; Laughlin, S. T.; Agard, N. J.; Chang, P. V.; Miller, I. A.; Lo, A.; Codelli, J. A.; Bertozzi, C. R. *Proc. Natl. Acad. Sci. U.S.A.* **2007**, *104* (43), 16793−16797.
(5) Jewett, J. C.; Bertozzi, C. R. *Chem. Soc. Rev.* **2010**, *39*, 1272−1279.
(6) Ess, D. H.; Jones, G. O.; Houk, K. N. *Org. Lett.* **2008**, *10* (8), 1633−36.
(7) Milner, S. T.; Witten, T. A.; Cates, M. E. *Macromolecules* **1988**, *21* (8), 2610−2619.
(8) Kumar, V.; Prud'homme, R. K. *J. Pharm. Sci.* **2008**, *97* (11), 4904−14.
(9) (a) Jose, J.; Burgess, K. *Tetrahedron* **2006**, *62*, 11021−11037. (b) Reichardt, C. *Chem. Rev.* **1994**, *94*, 2319−2358.
(10) Han, J.; Zhu, Z.; Qian, H.; Wohl, A. R.; Beaman, C. J.; Hoye, T. R.; Macosko, C. W. *J. Pharm. Sci.* **2012**, *101* (10), 4018−4023.
(11) (a) Dong, D. C.; Winnik, M. *Photochem. Photobiol.* **1982**, *35*, 17−21. (b) Zhao, C. L.; Winnik, M. A.; Riess, G.; Croucher, M. D. *Langmuir* **1990**, *6* (2), 514−516. (c) Luxenhofer, R.; Schulz, A.; Roques, C.; Li, S.; Bronich, T. K.; Batrakova, E. V.; Jordan, R.; Kabanov, A. V. *Biomaterials* **2010**, *31*, 4972−4979.

DOI: 10.1021/acsmacrolett.5b00119
ACS Macro Lett. 2015, 4, 521−525